Supplementary Material

Major Elements of the CPCD Model and Parameters Used

Radiative processes:

S_0 to S_1 ground to first excited singlet excitation; stimulated emission (photobleaching) from S_1 to S_0; fluorescence from the S_1 (the fluorescence lifetime is modulated by the collision rate in the expanding plume, rising from a low value in the solid to that corresponding to a free gas phase molecule); S_1 to S_n excitation, where S_n is a singlet at the laser photon energy above the S_1. S_1 to ion excitation, if the ionization potential of a matrix-analyte complex lies below twice the photon energy.

Nonradiative, single center processes:

S_1 internal conversion to S_0. S_n internal conversion to S_1; conversion of excess energy in the S_1 to internal energy, if the photon energy is above the S_1 vibrationless level.

Two center excitonic processes:

$S_1 + S_1$ pooling to $S_0 + S_n$ and $S_1 + S_n$ pooling to a ground state ion pair.

Charge transfer processes:

Matrix ion + analyte neutral reaction to analyte ion and matrix neutral; positive-negative charge recombination for all possible pairs, releasing the equivalent of the IP as internal energy; positive and negative ion reactions are treated separately, and have different reaction free energies; charge transfer reactions are reversible; charge transfer rates have an Arrhenius form, the activation energy is calculated from the reaction free energy using a nonlinear relationship. The inverse reaction has a correspondingly different activation energy, taking into account the reaction free energy. Bimolecular rates are scaled by the collision rate in the expanding plume. Multiple charging of analytes is not included, since it is not generally significant for small analytes like those considered here.

Ablation plume phenomena:

The plume is modeled as an adiabatic expansion. Matrix properties (heat capacity ratio, molecular weight) determine the expansion characteristics, since analyte is present in low concentration. The virtual orifice from which the plume expands is the laser spot, which is taken to be uniformly illuminated. The sample is assumed to change completely from solid to fluid at a fixed temperature. No clusters or aggregates are included in the model presented here. They arise naturally in the molecular dynamics implementation of the CPCD.[1-3] Because the laser is attenuated with depth, top layers vaporize sooner than deeper layers. Since the layers expand supersonically, there is little mass or energy exchange between layers following vaporization.

Differential equations describing these phenomena are numerically integrated over sufficient simulated time that the ion populations become stable. Charge and mass balance are checked during the integration, which uses double precision, 5th order Runge-Kutta methods, with adaptive step size, and a truncation relative error limit of 10^{-8}, in the Igor Pro environment (Wavemetrics, Lake Oswego, Oregon, USA).

The model was initially developed for DHB matrix, which has been characterized more thoroughly than others, particularly in molecular beams.[4-7] The choices of parameters for that matrix have been discussed in detail elsewhere.[8-10] Key parameters and those which were modified to extend the model to CHCA and ClCCA are discussed in more detail below.

Solid state absorption spectrum and absorption cross sections

A decisive parameter is the absorptivity of the solid matrix material. There have been numerous reports of solid state matrix spectra, but the measurements are difficult and are only consistent in terms of general spectral form.[11-18] A universally observed effect is the dramatic broadening and red shift of the absorption band in the solid compared to dilute solution. The broadening is typically 50 nm or more, corresponding to about 4000 cm^{-1} or 0.5 eV. This is obviously due to intermolecular interactions in the solid which do not exist in the isolated molecules. It is these interactions which are also responsible for exciton mobility and pooling in the solid state. The absorption spectra are a direct demonstration that these interactions are quite strong, both motivating and supporting the CPCD

approach based on these phenomena.

The solid state spectra used here are those reported by Soltwisch.[16] These spectra are normalized. While extinction coefficients or cross sections can be readily derived from solution phase data, they are very difficult to measure directly in the solid state. As a result, there is no consensus on appropriate values for MALDI matrix materials. Here the solution spectra were used to estimate the solid state cross sections of CHCA and ClCCA, using DHB as a reference. They were then adapted slightly to fit the experimental data, as listed in Table 1.

As an independent check these absorption cross sections were found to give not only appropriate thresholds, but also peak MALDI temperatures, at normal fluences (below 10 mJ/cm^2 for CHCA and ClCCA). Temperatures have been investigated both via direct and indirect means. Direct measurements used time-dependent infrared emission.[15, 19] These suffer from rather large uncertainties because the infrared emissivities are unknown. However, estimated temperatures are 1000 K or below.

These estimates are broadly consistent with those obtained from indirect temperature measurements using unimolecular decay.[20-23] These studies are expected to be reasonably reliable since the indicator molecules have been well characterized. They found temperatures of less than 1000 K, which is also consistent with limited quantities of matrix thermal decomposition products in the mass spectra, although some matrixes are known to be rather thermally labile.[24]

The largest fluences considered here are much higher than typically used in practice. The highest calculated temperatures are therefore also greater than normal. In principle, otherwise irrelevant thermal ionization mechanisms could become active at these temperatures. Such mechanisms are not included here. It will be shown that the CPCD alone is well able to reproduce the data, so superposing another model only confuses the issue, and is not applicable to typical conditions.

First excited electronic singlet state

The S_1 electronic origin of free DHB is at 357.69 nm,[4] and the fluorescence lifetime in a

cold molecular beam 30 ns. The lifetime in the solid state is less than 1 ns.[15, 25-28] The fluorescence decay is nonexponential, with an initial component of about 0.65 ns.

For the cinnamic acid derivatives, the approximate position of the S_1 origin was taken to be the 5% intensity point on the red edge of the solution phase absorption spectra. The Tuszynski group has performed extensive ultrafast investigations of CHCA and sinapinic acid crystals.[27, 28] They concluded that these molecules undergo photodimerization, but the dimer is unstable and decays back to the monomers. Their extensive study of these processes included wavelength dependent time resolved photoluminescence. They showed that the CHCA monomer absorbs and emits at shorter wavelengths, and is characterized by an initial lifetime of about 20 ps, dominated by the kinetics of reaction to the photodimer. The photoproducts absorb and emit at longer wavelengths (the extended red side of the solid state spectrum), and have a longer lifetime, of about 1.8 ns. In addition to dimerization, exciton diffusion was also found necessary to fully explain the time-resolved data. Since exciton migration and annihilation has already been demonstrated in DHB,[25, 26] this aspect of the CPCD has been experimentally confirmed in two of the three matrixes modeled here.

Since ClCCA is closely related to CHCA, it was assumed to have largely similar properties. The lifetimes were reduced slightly compared to CHCA, assuming a moderate internal heavy atom effect.[29] No information is available on the intrinsic radiative lifetimes of CHCA or ClCCA. Their higher absorptivity implies a shorter lifetime than DHB, 25 ns was assumed. This parameter is needed to estimate the fluorescence quantum efficiency.

Properties of dimers or excimers of all three matrixes were estimated during refinement of the model. These will be discussed below as part of the comparison with experimental data.

Pooling parameters

S_1 exciton dynamics including pooling (annihilation) in DHB have been investigated in some detail by fluorescence quenching and trapping methods.[25, 26] The data of 27, 28 for CHCA give similar magnitudes for S_1 processes, to the extent they can be compared. These values were also used for ClCCA. It should be noted that Hoyer[27] did not observe exciton-

induced phenomena in DHB, but the excitation energies and exciton densities appear to have been too low for this effect to have become apparent.

S_1 + S_n pooling is much more difficult to investigate, and no data exists for the cinnamic acids. The previously determined DHB values were taken as a starting point and modified within a small range. Best agreement with the data was obtained with somewhat faster pooling than in DHB.

Phase change temperature

Sublimation temperatures have been approximately determined for a few matrixes, including DHB and CHCA.[30] 450 K was used for DHB, CHCA was taken to be about 10 K higher. The chloro derivative is assumed to be like CHCA.

Ionization potentials

The DHB free molecule ionization potential (IP) is precisely known: 64 979 cm^{-1}, or 8.0564 eV.[4] Ionization potentials are also known for a number of (DHB)n clusters.[6] These converge to a limit of about 7.8 eV at n=10.

Ab initio methods for estimating matrix IPs were investigated in a study of electron transfer in MALDI.[31] With linear scaling, simple 4-31G(d,p) Koopman IPs were found to be as accurate as calculations using much larger basis sets. Using this method, the CHCA IP was estimated to be 8.50 eV and that of the chloro derivative 9.12 eV

Proton affinities and charge transfer reactions

Under the assumption that the relevant charge transfer reactions are proton transfer between matrix and analyte, the proton affinities (PA) of the matrixes are an important factor. Soltwisch, et al calculated proton affinites for the matrixes they tested with ab initio methods. These have been measured some time ago for DHB and CHCA,[32, 33] that of ClCCA has also been recently determined.[23] However, for the results presented here, it is not the matrix PA which is directly relevant, but the charge transfer free energies, in both polarities, for reaction with the analyte. We investigate this factor by varying the reaction free energy, not by specifying the PAs of matrix and analyte separately. Unless otherwise noted, for CHCA and DHB, the positive charge transfer reaction energy was taken to be

-100 kJ/mol, while for ClCCA it was -125 kJ/mol. The negative reaction energy was -50 kJ/mol in all cases. These are not atypical values for these matrixes reacting with peptides.

The activation energy for charge transfer is derived from the reaction energy via the Agmon-Levine equation.[34, 35] The key parameter in that relationship, lambda, was originally chosen for DHB to be 15, a typical value for proton transfer reactions.[9] The analyte ion yields for CHCA and ClCCA were found in Ref. 16 to be lower than for DHB, as a fraction of the total ion current. This data was used to adjust the lambda factor for the new matrixes. Higher lambda values result in higher activation energies and lower reaction rates. A value of 30 is currently proposed for CHCA and ClCCA, as listed in Table 1.

Data Treatment

The experimental plots have a different appearance than in Soltwisch, et al. because a different procedure was used to generate them from the sparse data. The following figures illustrate the method, for CHCA.

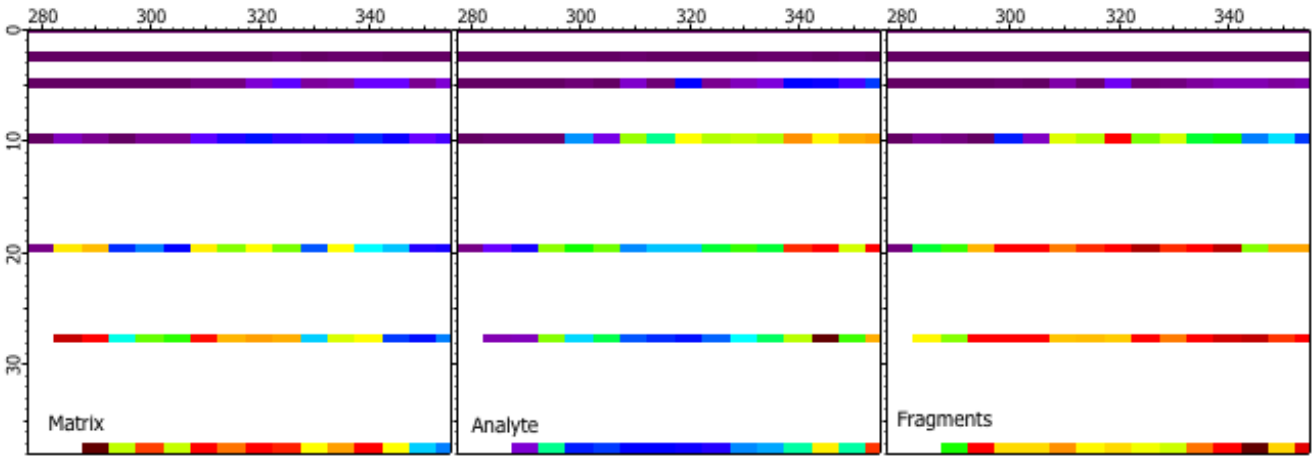

Figure S1. The raw data, as supplied by Soltwisch and Dreisewerd. The color scale is different for each, ranging in each case from the minimum to the maximum value. Fluence is on the left axis (mJ/cm^2) and wavelength on the top (nm).

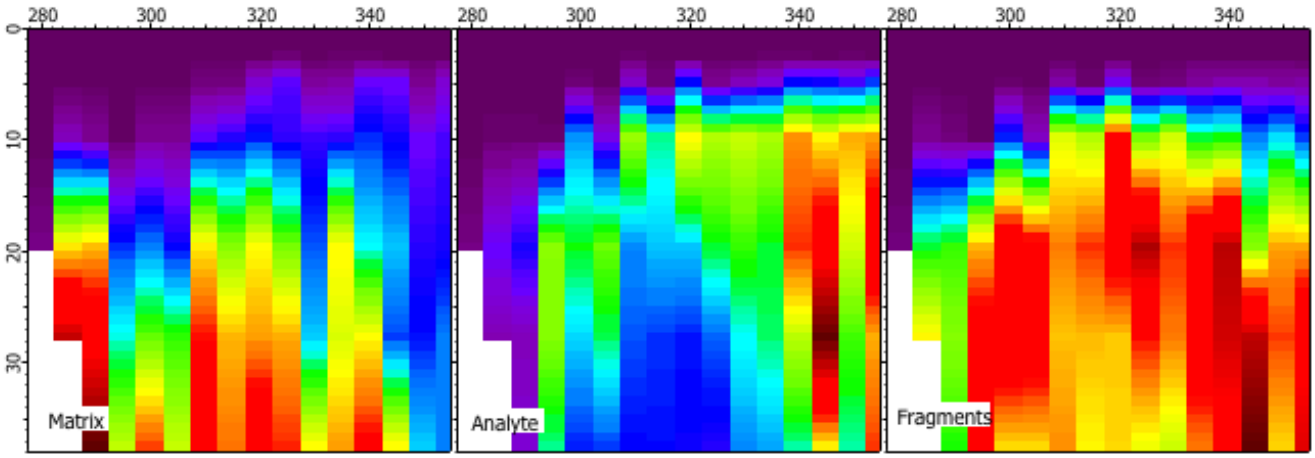

Figure S2. For each wavelength, the data were next linearly interpolated between the fluence points:

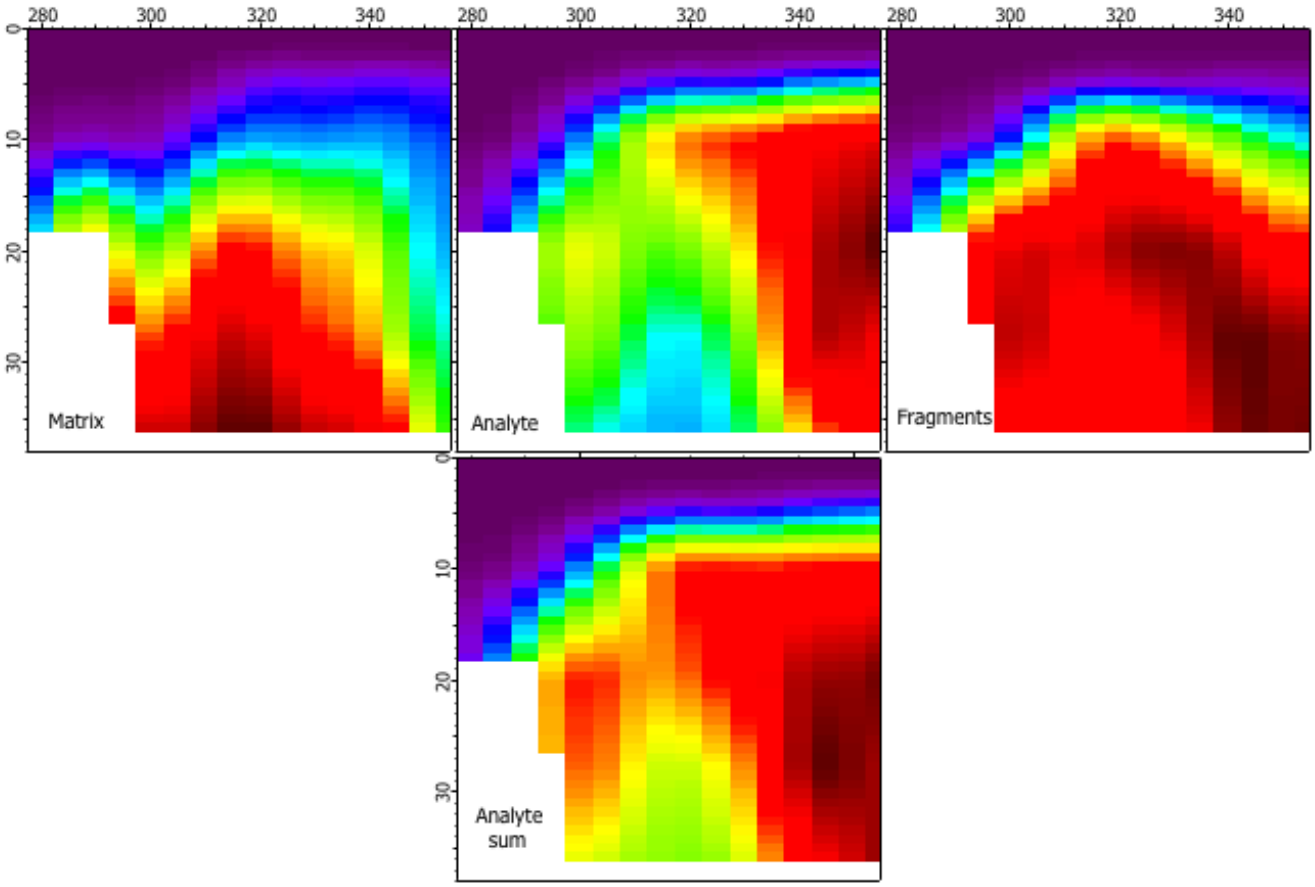

Figure S3. Finally, the data were smoothed using a 5x5 gaussian filter. The sum of the intact analytes and their fragments was compared to the CPCD.

Soltwisch, et al. used an interpolation procedure that was not restricted to the fluence axis. It attempts to find approximate contours of constant intensity. This has the disadvantage of potentially producing small scale features where none exist. On the other hand, it may sometimes prevent loss of real features that would be suppressed by, for example, smoothing.

Analyte Fragmentation

It was concluded by Soltwisch, et al. that analyte fragmentation was largely thermal, rather than photoinduced. However, comparison of the distribution of analyte fragments with the calculated temperatures suggests that some non-thermal process might be contributing, particularly in for CHCA matrix.

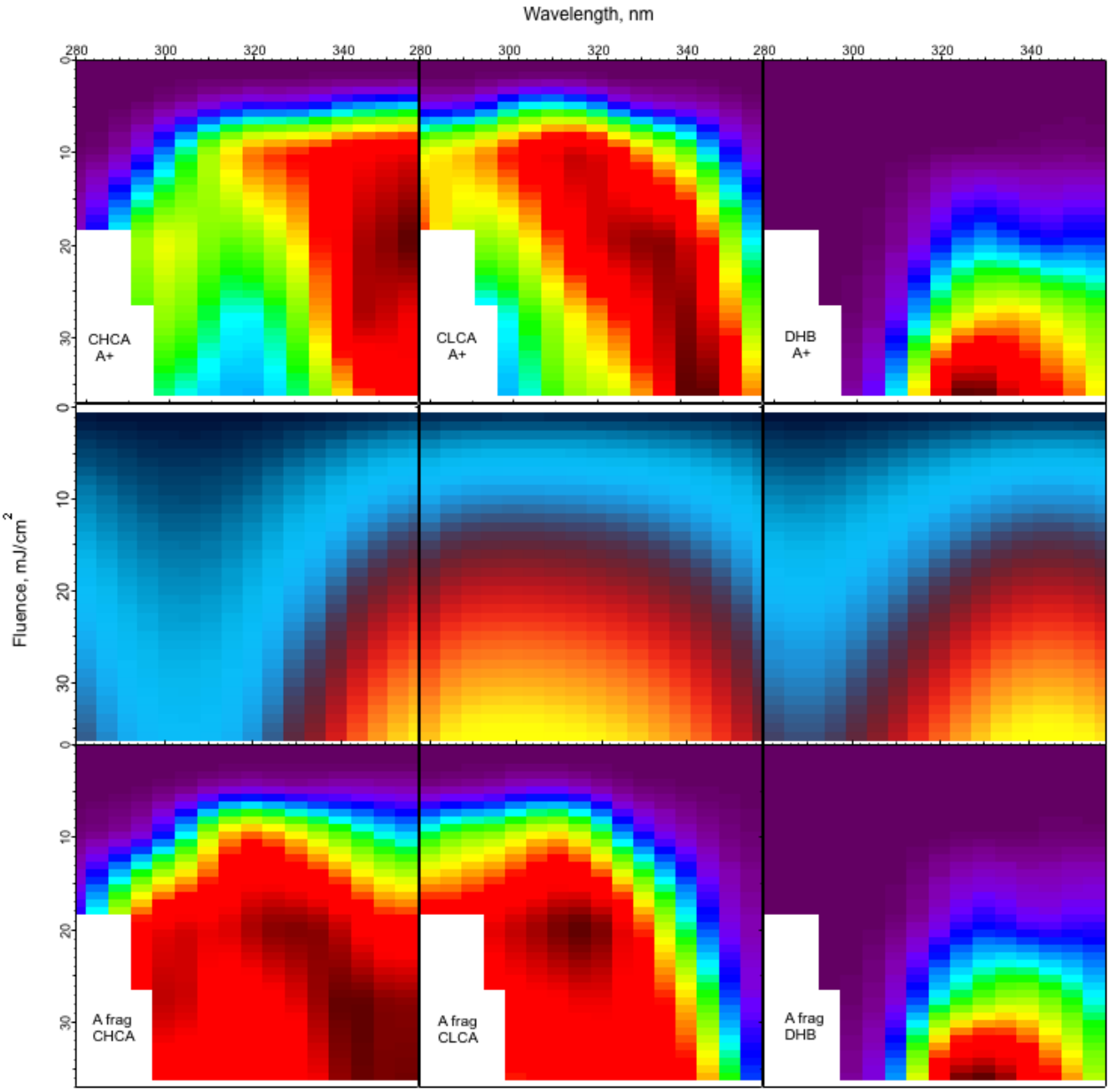

Figure S4. The intact analyte and analyte fragment data of Soltwisch, et al. are compared to the thermal distributions of Fig. 6 in the main text.

Depth Integration

As noted in the text, and in agreement with Soltwisch, et al., the experimental data are believed to largely reflect ions emitted from the uppermost layer(s) of the sample. The CPCD calculations were performed accordingly. The CPCD can also be used in a depth-integrating mode. The sample is divided into thin layers, the thicknesses are adjusted for constant laser energy deposition (thinner at the surface). Each layer is calculated and the results summed. The number of layers was increased until no change in the results was observed. In the following figure, 150 layers were specified.

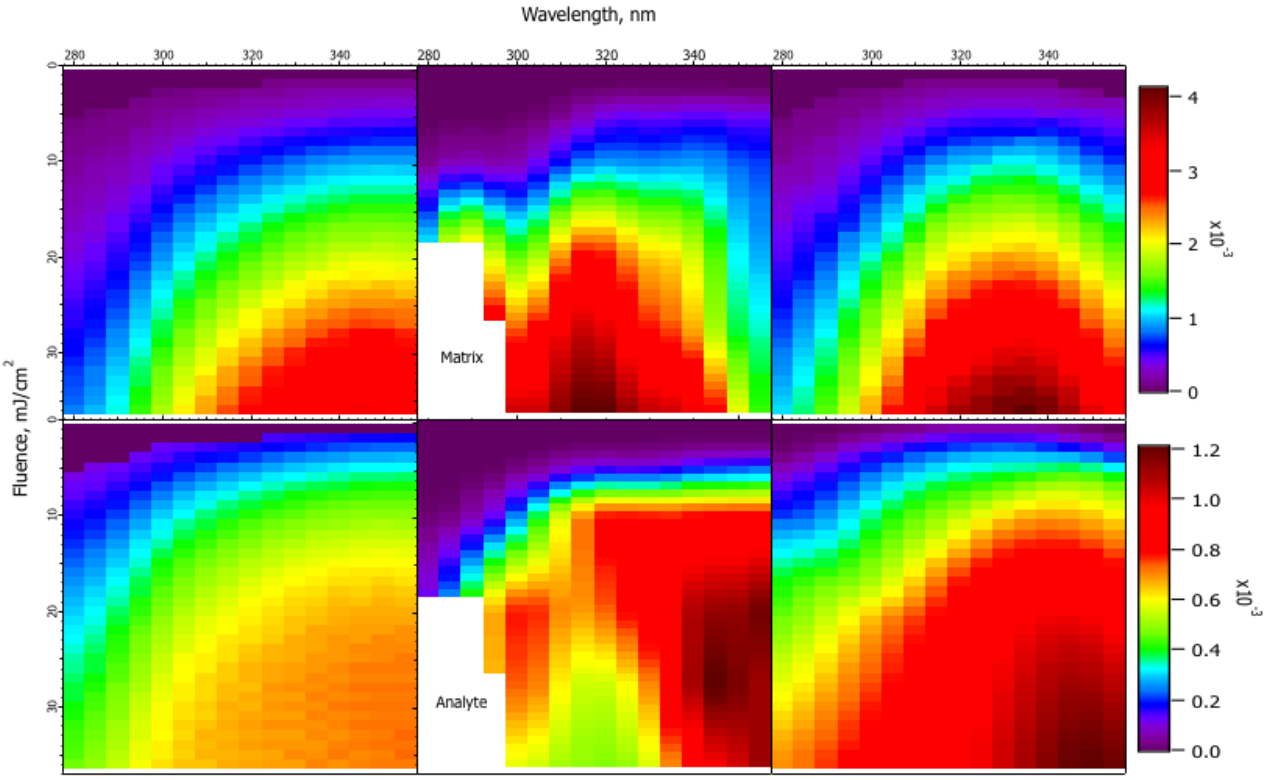

Figure S5. Depth-integrated CPCD results for CHCA matrix. These results should be compared with the top layer results of Figure 3 in the text. Depth integration smears out finer structure in the plots.

Charge Transfer Energetics

The free energies of reaction of primary matrix ions with analytes are assumed in the CPCD to modulate the rate of reaction, via a non-linear free energy relationship (see above). As reported in the main text, typical values of the reaction energies give good agreement with the data. Large values than in the text have relatively small effects. The next figure illustrates that low reaction energies change the fluence-wavelength plots noticeably.

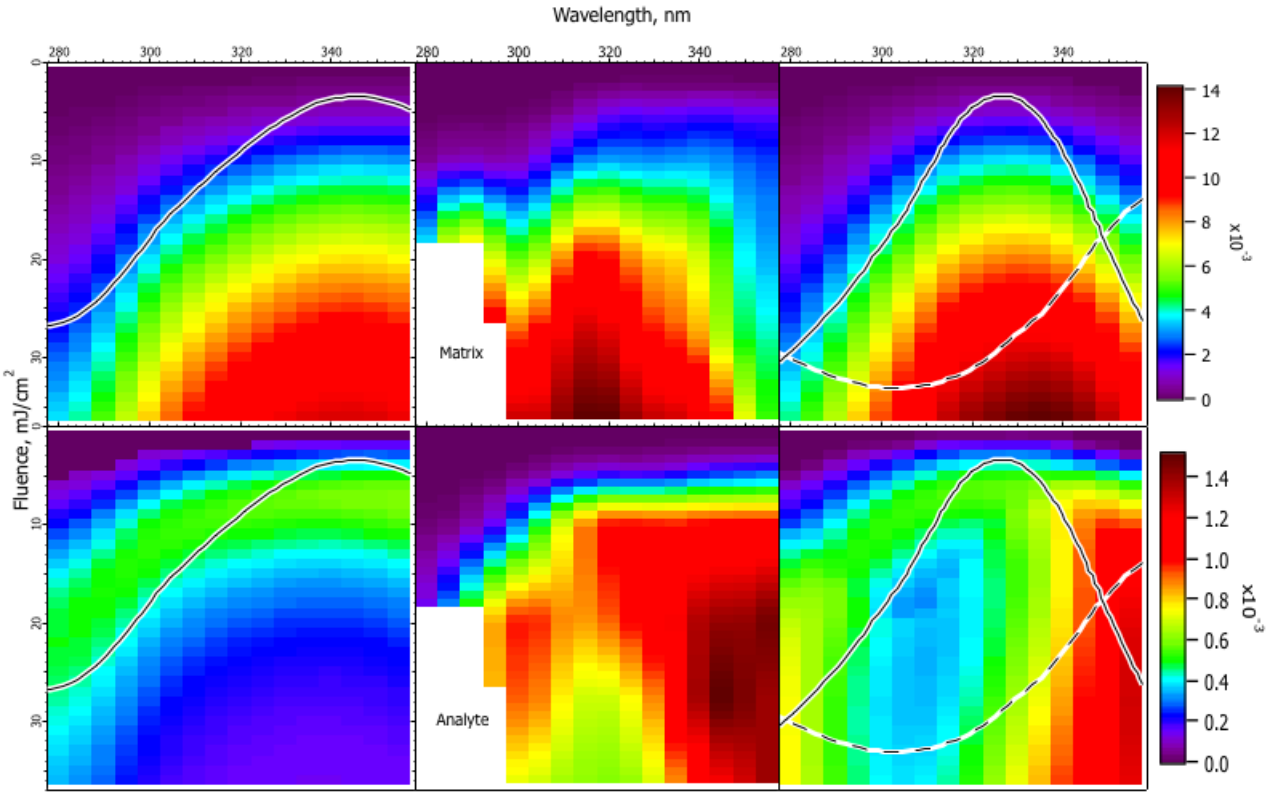

Figure S6. Fluence vs wavelength plots for CHCA matrix. The experimental data of Ref. 16 are in the middle. The calculated results are as in Fig. 3, except that the positive charge transfer reaction free energy was ΔG=-50 kJ/mol. The ion yield color scales (mol/mol) apply to the calculated results in their respective rows, not to the experimental data.

Analyte Relative Ion Yields

Total analyte fractional yields included also the fragment yields. The CPCD results are calculated with lambda=30, as described in the text.

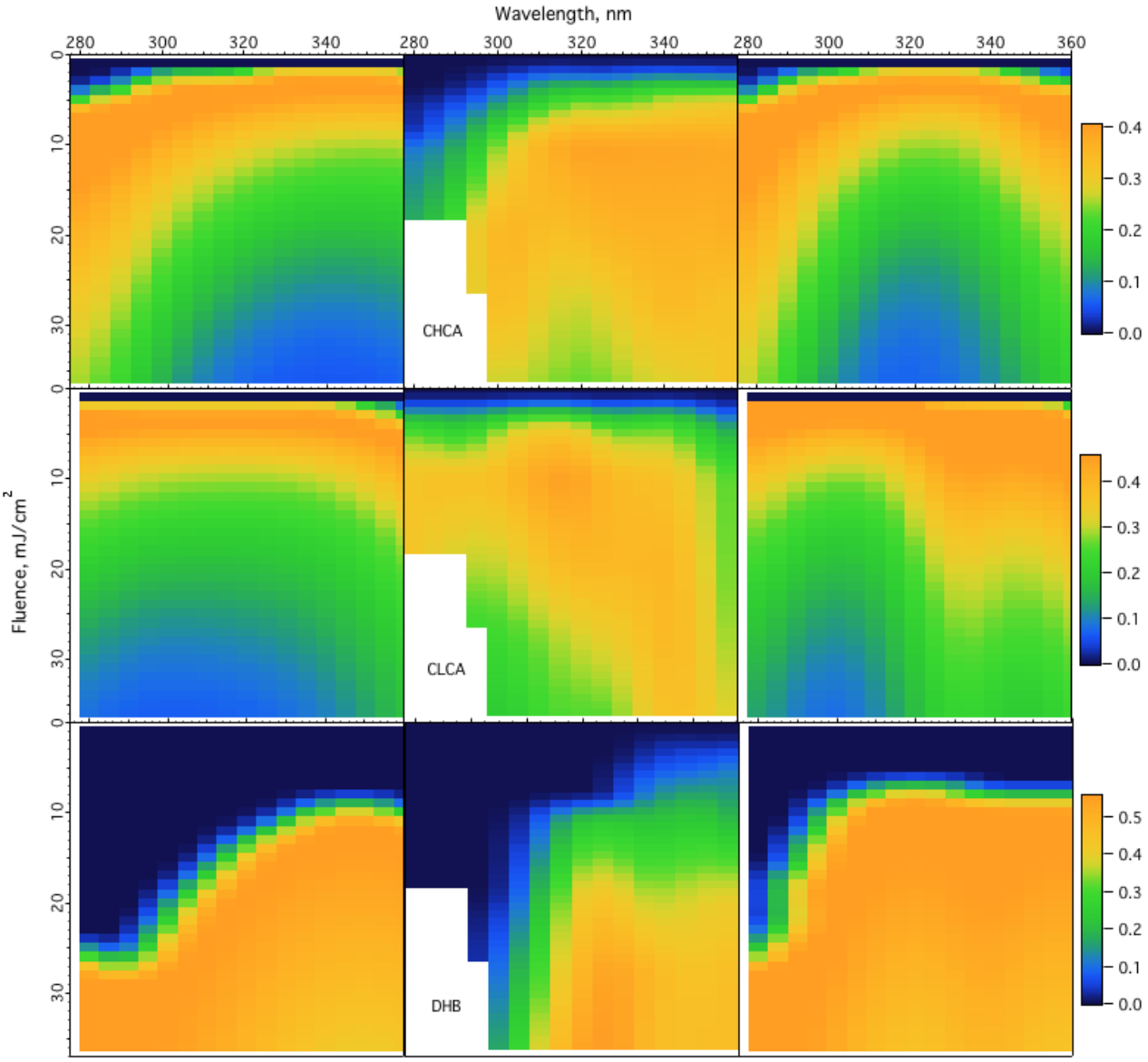

Figure S7. Analyte ion yield relative to total ion production (mol/mol), as calculated by the CPCD and compared to the data of Soltwisch et al. The experimental data are in the middle column, CPCD results using the solid state spectrum are in the left column, while the summed monomer plus dimer / excimer are in the right column.

References

1. R. Knochenmuss, L. V. Zhigilei, *J. Phys. Chem. B,* 2005, **109,** 22947-229957.
2. R. Knochenmuss, L. V. Zhigilei, *J. Mass Spectrom.,* 2010, **45,** 333-346.
3. R. Knochenmuss, L. V. Zhigilei, *Anal. Bioanal. Chem.,* 2012, **402,** 2511-2519.
4. V. Karbach, R. Knochenmuss, *Rapid Commun. Mass Spectrom.,* 1998, **12,** 968-974.
5. G. Kinsel, R. Knochenmuss, P. Setz, C. M. Land, S.-K. Goh, E. F. Archibong, J. H. Hardesty, D. Marynick, *J. Mass Spectrom.,* 2002, **37,** 1131-1140.
6. Q. Lin, R. Knochenmuss, *Rapid Comm. Mass Spectrom.,* 2001, **15,** 1422-1426.
7. W. E. Wallace, M. A. Arnould, R. Knochenmuss, *Int. J. Mass Spectrom.,* 2005, **242,** 13-22.
8. R. Knochenmuss, *J. Mass Spectrom.,* 2002, **37,** 867-877.
9. R. Knochenmuss, *Anal. Chem.,* 2003, **75,** 2199.
10. R. Knochenmuss, *Int. J. Mass Spectrom.,* 2009, **285,** 105-113.
11. D. A. Allwood, R. W. Dreyfus, I. K. Perera, P. E. Dyer, *Rapid Commun. Mass Spectrom.,* 1996, **10,** 1575-1578.
12. D. A. Allwood, R. W. Dreyfus, I. K. Perera, P. E. Dyer, *Appl. Surf. Sci.,* 1997, **110,** 154-157.
13. T. Porta, C. Grivet, R. Knochenmuss, E. Varesio, G. Hopfgartner, *J. Mass Spectrom.,* 2011, **46,** 144-152.
14. J. R. Haulenbeek, PhD Dept of Chemistry, Drexel University, Philadelphia (2012).
15. Y.-H. Lai, C.-C. Wang, C. W. Chen, B.-H. Liu, S. H. Lin, Y. T. Lee, *J. Phys. Chem. B,* 2012, **116,** 9635-9643.
16. J. Soltwisch, T. W. Jaskolla, F. Hillenkamp, M. Karas, K. Dreisewerd, *Anal. Chem.,* 2012, **84,** 6567-6576.
17. H. Ehring, C. Costa, P. A. Demirev, B. U. R. Sundqvist, *Rapid Commun. Mass Spectrom.,* 1996, **10,** 821-824.
18. T. W. Heise, E. S. Yeung, *Anal. Chim. Acta,* 1995, **199,** 377 - 385.
19. A. Koubenakis, V. Frankevich, J. Zhang, R. Zenobi, *J. Phys. Chem. A,* 2004, **108,** 2405-2410.
20. G. Luo, I. Marginean, A. Vertes, *Anal. Chem.,* 2002, **74,** 6185-6190.
21. V. Gabelica, E. Schulz, M. Karas, *J. Mass Spectrom.,* 2004, **39,** 579-593.
22. Y. J. Bae, J. H. Moon, M. S. Kim, *J. Am. Soc. Mass Spectrom.,* 2011, **22,** 1070-1078.

23. T. W. Jaskolla, W. D. Lehmann, M. Karas, *Proc. Nat. Acad. Sci. U.S.A.,* 2008, **105,** 12200-12205.
24. O. I. Tarzi, H. Nonami, R. Erra-Balsells, *J. Mass Spectrom.,* 2009, **44,** 260-277.
25. P. Setz, R. Knochenmuss, *J. Phys. Chem. A,* 2005, **109,** 4030-4037.
26. H.-C. Lüdemann, R. W. Redmond, F. Hillenkamp, *Rapid Comm. Mass Spectrom.,* 2002, **16,** 1287-1294.
27. T. Hoyer, Dr. rer. nat. Faklutät für Mathematik und Naturwissenschaften, Carl von Ossietzky Universität Oldenburg, Oldenburg (2009).
28. T. Hoyer, W. Tuszynski, C. Lienau, *Chem. Phys. Lett.,* 2007, **443,** 107-112.
29. L. M. Preston-Schaffter, G. R. Kinsel, D. H. Russell, *J. Am. Soc. Mass Spectrom.,* 1994, **5,** 800-806.
30. E. Stevenson, K. Breuker, R. Zenobi, *J. Mass Spectrom.,* 2000, **35,** 1035-1041.
31. A. J. Hoteling, W. F. Nichols, D. J. Giesen, J. R. Lenhard, R. Knochenmuss, *Eur. J. Mass Spectrom.,* 2006, **12,** 345-358.
32. T. J. D. Jørgensen, G. Bojesen, H. Rahbek-Nielsen, *Eur. Mass Spectrom.,* 1998, **4,** 39-45.
33. R. D. Burton, C. H. Watson, J. R. Eyler, G. L. Lang, D. H. Powell, M. Y. Avery, *Rapid Commun. Mass Spectrom.,* 1997, **11,** 443-446.
34. N. Agmon, *Int. J. Chem. Kin.,* 1981, **13,** 333-365.
35. N. Agmon, R. D. Levine, *Israel J. Chem.,* 1980, **19,** 330-336.